ChemComm

COMMUNICATION

View Article Online
View Journal | View Issue

Star block-copolymers: enzyme-inspired catalysts for oxidation of alcohols in water†

Cite this: *Chem. Commun.*, 2014, **50**, 7862

Received 6th May 2014,
Accepted 23rd May 2014

DOI: 10.1039/c4cc03370a

www.rsc.org/chemcomm

Clément Mugemana, Ba-Tian Chen, Konstantin V. Bukhryakov and Valentin Rodionov*

Published on 30 May 2014. Downloaded by Aston University on 25/08/2014 21:46:56.

A number of fluorous amphiphilic star block-copolymers containing a tris(benzyltriazolylmethyl)amine motif have been prepared. These polymers assembled into well-defined nanostructures in water, and their mode of assembly could be controlled by changing the composition of the polymer. The polymers were used for enzyme-inspired catalysis of alcohol oxidation.

Nature's enzymes are complex polymer catalysts that are capable of facilitating thousands of challenging reactions with perfect fidelity and selectivity. This exquisite level of functionality is achieved through precise, programmed folding into intricate tertiary structures[1] and close participation of cofactors, prosthetic groups and metal ions. Often, the active sites and cofactor binding pockets are separated from the bulk aqueous phase and buried in the hydrophobic interior of the protein.

Recent publications explored the use of chemist-made macromolecules, either branched[2,3] or single-chain,[4] as enzyme-inspired catalysts. Rational design of linear polymers with protein-like tertiary or quaternary structures and catalytic function remains an elusive (but tantalizing) goal.[5] Materials with branched topologies are amenable to structural engineering, at the cost of greater synthetic complexity (dendrimers) or increased heterogeneity (star polymers).

In this study, we present a pathway to enzyme-inspired catalytic materials based on star block-copolymers with limited branching. These polymers incorporate hydrophilic, superhydrophobic, and polydentate metal-binding characteristics. The interplay of these structural characteristics determines the mode of self-assembly and the catalytic competence of the macromolecules.

The Cu/TEMPO (2,2,6,6-tetramethyl-1-piperidine-*N*-oxyl) system, introduced by Semmelhack[6] in 1984 and further developed by Sheldon,[7] Stahl[8] and others,[9] has emerged as one of the most attractive catalysts for selective aerobic oxidation of primary alcohols.[10] The established protocols for Cu/TEMPO catalyzed alcohol oxidation strongly favor organic solvents, especially acetonitrile.[8] We aimed to design an enzyme-inspired functional macromolecular architecture that could enable the transfer of this catalytic system to pure water. Such a transfer could enable large-scale applications of Cu/TEMPO, while circumventing the usual safety concerns associated with combining oxygen and organic solvents.

We envisioned that amphipolar, globular assemblies, with metal-binding sites buried inside hydrophobic cores (Fig. 1a), could provide the necessary site isolation of the catalytic metal centers.[11] However, the accumulation of hydrophobic reaction products inside such assemblies would be undesirable, as the transfer of an additional alcohol substrate to the active site would be hindered. To avoid this potential problem, we chose "everything-phobic" fluorous monomers as building blocks for the cores of our prospective catalysts.[12,13] Understanding that perfluorocarbons and their emulsions in water are capable of dissolving substantial amounts of O_2,[14,15] we reasoned that a fluorous core of a polymer globule could pre-concentrate oxygen in the vicinity of the active metal site.

We selected the tris(benzyltriazolylmethyl) amine (TBTA) motif[16] as a metal-binding site, due to its ability to stabilize the Cu^I oxidation state, its versatile coordination chemistry[17] (Fig. 1b), and its easy synthetic accessibility. Starting with the TBTA-based polymerization initiator **1** (Fig. 1c), we proceeded to synthesize a number of superhydrophobic three-arm polymers *via* nitroxide-mediated polymerization (NMP).[18] We chose this mode of polymerization over synthetically simpler atom-transfer radical polymerization,[19] as the latter can be affected by the presence of Cu^I binding sites in the target polymers.

Pentafluorostyrene (PFS), 2,2,3,3,4,4,4-heptafluorobutyl acrylate (PFBA) and 1*H*,1*H*,2*H*,2*H*-perfluorodecyl acrylate (PFDA) were polymerized with initiator **1**, either in the bulk or in cyclohexanone at 120 °C. For each fluorinated monomer, we aimed to create at least two macroinitiators with different degrees of polymerization (DP) to evaluate the effects of the hydrophobic core size on catalytic

---

KAUST Catalysis Center and Division of Physical Sciences and Engineering, King Abdullah University of Science and Technology, Thuwal, 23955-6900, Kingdom of Saudi Arabia. E-mail: valentin.rodionov@kaust.edu.sa; Tel: +966 (12) 8084592

† Electronic supplementary information (ESI) available: Experimental details for polymer and organic synthesis; characterization (^{1}H, ^{13}C, and ^{19}F NMR, FTIR spectra). See DOI: 10.1039/c4cc03370a

This journal is © The Royal Society of Chemistry 2014

Published on 30 May 2014. Downloaded by Aston University on 25/08/2014 21:46:56.

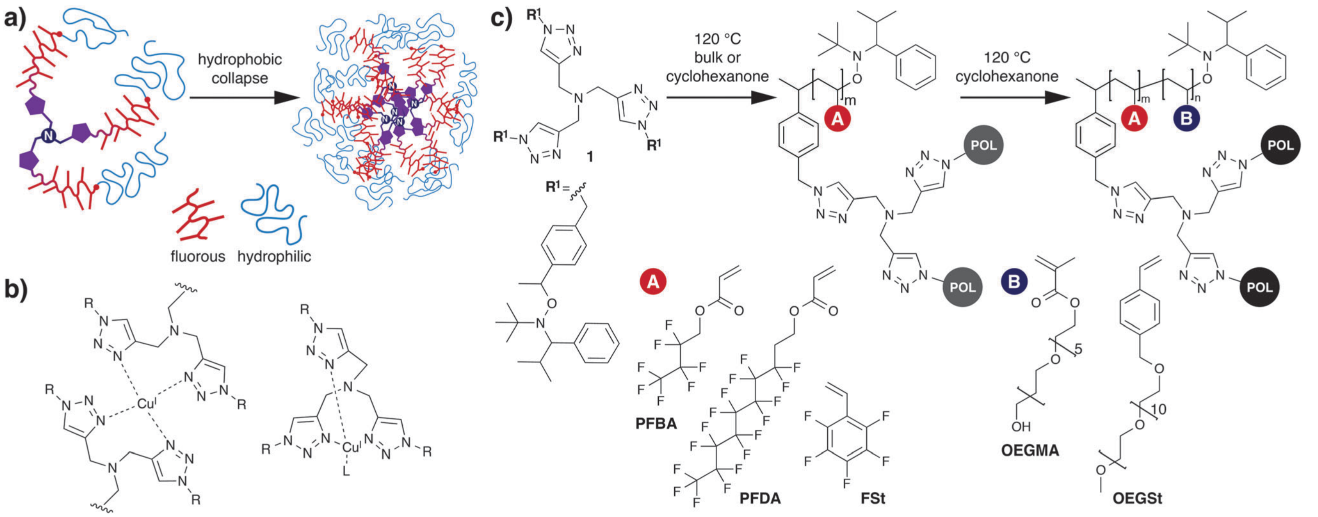

Fig. 1 (a) Design for an amphiphilic block copolymer micelle with metal binding sites at the core. (b) Some of the modes of coordination possible for a TBTA-type ligand. (c) Synthesis of amphiphilic star block copolymers.

competency (Table S3, ESI†). A DP higher than 4 could not be reached for PFDA due to the anomalously low solubility of resulting polymers.

The hydrophobic macroinitiators were used for the polymerization of two hydrophilic monomers, *p*-oligo(ethylene glycol) styrene (OEGSt) and oligo(ethylene glycol) methacrylate (OEGMA). OEGSt was polymerized in cyclohexanone, leading to a range of amphiphilic star copolymers (Table 1, entries 1–5). Although NMP is rarely a polymerization of choice for methacrylates,[20] we obtained a higher DP for the copolymerization of OEGMA than we did for styrenic OEGSt (Table 1, entries 6–9). Size exclusion chromatography (SEC) on all the copolymerization reactions indicated a clean shift of population towards a higher number-average molecular weight (M_n), with little to no tailing (although limited aggregation was observed for (PFDA$_4$-*b*-OEGSt$_4$)$_3$ and (PFBA$_{20}$-*b*-OEGSt$_4$)$_3$).

We investigated the self-assembly modes of the copolymers by obtaining cryogenic transmission electron microscopy (cryo-TEM) and atomic force microscopy (AFM) images of their aggregates. Spherical aggregates with diameters between 20 and 50 nm were the main type of assemblies for (PFS$_7$-*b*-OEGSt$_3$)$_3$, (PFS$_{10}$-*b*-OEGSt$_4$)$_3$, (PFBA$_7$-*b*-OEGMa$_{18}$)$_3$, (PFBA$_{14}$-*b*-OEGMa$_{30}$)$_3$, (PFDA$_4$-*b*-OEGMa$_{30}$)$_3$, and (PFS$_{16}$-*b*-OEGMA$_{30}$)$_3$ (Fig. 2a–c, and Sections 4.6–7, ESI†). AFM phase images (Fig. 2b and Section 4.6, ESI†) revealed the separation between the hydrophobic aggregate cores and hydrophilic coronas. The size of the aggregates observed was consistent between cryo-TEM and AFM, taking into account the flattening/spreading of the soft material on the substrate (Table 1 and Table S2, ESI†).

We found that by increasing the weight fraction of the fluorinated block in the copolymer, more complex morphologies could be triggered. The (PFBA$_{20}$-*b*-OEGSt$_4$)$_3$ copolymer, which contains 67 wt% of the fluorous monomer, assembled into well-defined vesicles, unilamellar (Fig. 2f), as well as multilamellar (Fig. 2g). The thickness of the vesicle boundaries was *ca.* 9 nm, which suggests that they were formed by a single layer of macromolecules. The AFM image of (PFBA$_{20}$-*b*-OEGSt$_4$)$_3$ showed that some vesicles remain intact even in the partially dry state. Objects with diameters ranging from *ca.* 60 to 120 nm and with heights from 30 to 40 nm were observed. In addition to the aggregates with pronounced height, flat structures of similar lateral dimensions could be seen (Fig. 2d–e). We presume that some of the vesicles retain their interior water when

Table 1 Characterization of amphiphilic star block copolymers

Entry	Polymer[a]	M_n[b]	M_w[b]	PDI$_{SEC}$	DLS[c] (nm)	PDI$_{DLS}$	AFM[d] (nm)	TEM (nm)
1	(PFS$_7$-*b*-OEGSt$_3$)$_3$	5900	6600	1.12	20(90%)/160(10%)	0.23	76 ± 10	20 ± 2[f]
2	(PFS$_{10}$-*b*-OEGSt$_4$)$_3$	11 200	13 216	1.18	28(30%)/135(70%)	0.22	44 ± 6	26 ± 2[f]
3	(PFS$_{16}$-*b*-OEGSt$_4$)$_3$	12 400	15 130	1.22	70(70%)/130(30%)	0.24	46 ± 4	42 ± 4[e]
4	(PFBA$_{20}$-*b*-OEGSt$_4$)$_3$	12 800	16 400	1.28	70	0.36	100 ± 14	120–350[f]
5	(PFDA$_4$-*b*-OEGSt$_4$)$_3$	11 500	14 720	1.28	20(90%)/140(10%)	0.54	74 ± 4	22 ± 1[f]
6	(PFS$_{16}$-*b*-OEGMA$_{30}$)$_3$	13 500	16 470	1.22	120(42%)/200(58%)	0.22	70 ± 6	44 ± 8[f]
7	(PFBA$_7$-*b*-OEGMA$_{18}$)$_3$	11 230	13 360	1.19	30(48%)/300(52%)	0.28	70 ± 8	58 ± 10[e]
8	(PFBA$_{14}$-*b*-OEGMA$_{30}$)$_3$	13 200	15 970	1.21	30(89%)/250(11%)	0.29	88 ± 4	52 ± 10[e]
9	(PFDA$_4$-*b*-OEGMA$_{30}$)$_3$	11 000	12 320	1.12	40(86%)/255(14%)	0.44	76 ± 10	24 ± 4[f]

[a] Degree of polymerization determined by ^{1}H NMR. [b] Determined by SEC (calibration against linear polystyrene). [c] Hydrodynamic diameters determined by dynamic light scattering (DLS) in water at 1 g L^{-1}. For multimodal distributions, diameters are estimated based on intensity distribution, and relative ratios based on volume distribution. [d] Diameters of aggregates determined from AFM height images. [e] Diameter of aggregates determined from TEM images. [f] Diameter of aggregates determined from cryo-TEM images.

Published on 30 May 2014. Downloaded by Aston University on 25/08/2014 21:46:56.

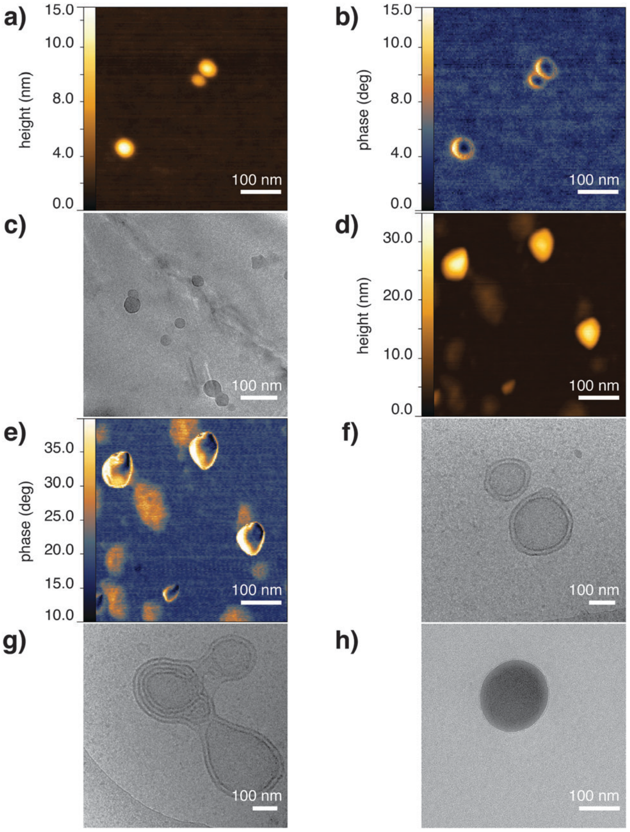

Fig. 2 (a) and (b) AFM height and phase images of $(PFS_{16}\text{-}b\text{-}OEGMA_{30})_3$ block copolymer micelles spin-coated onto a Si substrate. (c) Cryo-TEM image of $(PFS_{16}\text{-}b\text{-}OEGMA_{30})_3$ block copolymer micelles in water. (d) and (e) AFM height and phase images of $(PFBA_{20}\text{-}b\text{-}OEGSt_4)_3$ vesicular structures. (f) and (g) Cryo-TEM images of $(PFBA_{20}\text{-}b\text{-}OEGSt_4)_3$ vesicular structures, unilamellar and multilamellar. (h) Cryo-TEM image of a $(PFBA_{20}\text{-}b\text{-}OEGSt_4)_3$ vesicle in the presence of $CuSO_4$.

deposited on the substrate, while others "deflate" and spread. Unlike spherical aggregates, the "deflated" vesicles show no core–corona contrast in the AFM phase image. The vesicular structures persisted after addition of $CuSO_4$. A significant amount of Cu was sequestered in the vesicle's boundary, as evidenced by the increased contrast in the cryo-TEM image (Fig. 2h).

Examination of aqueous polymer solutions by DLS (Section 4.5, ESI†) revealed 20–70 nm aggregates in agreement with AFM and TEM images, as well as larger species with hydrodynamic diameters varying from *ca.* 100 to 300 nm. It is likely that the larger species are not abundant enough to feature prominently in TEM images, and unravel/disassemble when spread on AFM substrates. Much smaller, 5–20 nm species were observed in the polymer solutions prepared in good organic solvents, such as DMF and THF (Fig. S41–S42, ESI†).

The catalytic competency of the star polymers was evaluated for a Cu/TEMPO-catalyzed alcohol oxidation reaction, using a modification of the protocol originally reported by Stahl.[8] Polymers were dispersed in water, the "cofactors" TEMPO and 4-dimethylaminopyridine (DMAP) were added, and the solutions were treated with ultrasound. $CuSO_4$ and benzyl alcohol were added to start the reaction. The rate of oxidation was negligible in the absence of the star polymers (Table 2, entries 1 and 2). Addition of PFS and PFDA copolymers led to a marginal improvement of reaction yields (Table 2, entries 3, 5 and 7). To our delight, the TEMPO–Cu system became catalytically competent in the presence of star polymers with PFBA hydrophobic cores (Table 2, entries 4, 6 and 8). The nature of the hydrophilic monomer, the degree of polymerization, or the weight fraction of the fluorinated monomer had little influence on the catalytic competency: $(PFBA_{20}\text{-}b\text{-}OEGSt_4)_3$, $(PFBA_7\text{-}b\text{-}OEGMA_{18})_3$, and $(PFBA_{14}\text{-}b\text{-}OEGMA_{30})_3$ were similar in their capacity for catalyzing alcohol oxidation. Upon further optimization of reaction conditions (Table 2, entries 9–12), an almost quantitative yield of benzaldehyde was obtained in the presence of $(PFBA_{14}\text{-}b\text{-}OEGMA_{30})_3$.

The capacity of the polymers to pre-concentrate molecular oxygen was assessed next. Polymer solutions (2 wt%) were saturated with O_2 by vigorous shaking in vials in an atmosphere of pure oxygen. Following this, the vial headspace was vented, and the concentration of O_2 in solution was measured in 5 min

Table 2 Catalytic oxidation of benzyl alcohol in the presence of block-copolymer micellar aggregates

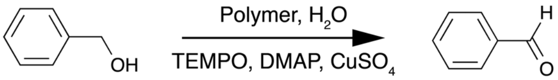

Entry	Block copolymer	Time [h]	TEMPO[a] [mol%]	DMAP[a] [mol%]	$CuSO_4$[a] [mol%]	Polymer [wt%]	Conversion[b] [%]
1	—	36	1	5	0.2	—	<1
2	—	44	2.5	50	2	—	5
3	$(PFS_{10}\text{-}b\text{-}OEGSt_4)_3$	36	1	5	0.2	0.04	6
4	$(PFBA_{20}\text{-}b\text{-}OEGSt_4)_3$	36	1	5	0.2	0.04	28
5	$(PFS_{16}\text{-}b\text{-}OEMa_{30})_3$	36	1	5	0.2	0.04	5
6	$(PFBA_7\text{-}b\text{-}OEGMa_{18})_3$	36	1	5	0.2	0.04	25
7	$(PFDA_4\text{-}b\text{-}OEGMa_{30})_3$	36	1	5	0.2	0.04	6
8	$(PFBA_{14}\text{-}b\text{-}OEGMa_{30})_3$	36	1	5	0.2	0.04	22
9	$(PFBA_{14}\text{-}b\text{-}OEGMA_{30})_3$	37	2.5	25	4	3.11	46
10	$(PFBA_{14}\text{-}b\text{-}OEGMA_{30})_3$	31	2.5	25	2	1.56	53
11	$(PFBA_{14}\text{-}b\text{-}OEGMA_{30})_3$	21	5	25	2	1.27	61
12	$(PFBA_{14}\text{-}b\text{-}OEGMA_{30})_3$	44	2.5	50	2	1.56	90

[a] Relative to benzyl alcohol. [b] Determined by ^1H NMR.

This journal is © The Royal Society of Chemistry 2014

Published on 30 May 2014. Downloaded by Aston University on 25/08/2014 21:46:56.

intervals using an Inlab 605 probe (Mettler Toledo). For both pure water and $(PFS_{16}\text{-}b\text{-}OEGSt_4)_3$ solution, the dissolved O_2 concentration dropped to its air-saturated value of ~9 mg L^{-1} in ~25 min (Fig. S69, ESI†). Similar equilibration kinetics was observed for the 2 wt% solution of Pluronic P123. Since Pluronic solutions are prone to foaming, the slightly slower O_2 release in this case compared to pure water can be attributed to gas retention in foam bubbles. The behavior of the $(PFBA_{14}\text{-}b\text{-}OEGMA_{30})_3$ solution was markedly different. After 30 min, the dissolved O_2 concentration was still ~20 mg L^{-1}, which is approximately 200% of air-saturated concentration in pure water. This suggests that the catalytic competency of amphiphilic PFBA copolymers is due to their capacity to attract and pre-concentrate O_2 in the hydrophobic environment surrounding the metal-binding site.

In conclusion, we prepared a library of well-defined star block-copolymers from a trifunctional nitroxide initiator based on the TBTA motif. In water, the copolymers self-assemble into micelles or vesicles, depending on the specific polymer composition. Copolymers containing PFBA monomers show evidence of molecular oxygen pre-concentration in the fluorinated cores of their micellar aggregates. In combination with DMAP and TEMPO "cofactors" and in the presence of $CuSO_4$, these copolymers act as competent catalysts for oxidation of alcohols to aldehydes in water.

Authors are grateful to Prof. Nikos Hadjichristidis for helpful discussions. Funding from KAUST OCRF (award project "Catalysis with Soft Materials") is acknowledged with thanks.

Notes and references

1 A. Fersht, *Structure and Mechanism in Protein Science: A Guide to Enzyme Catalysis and Protein Folding*, W. H. Freeman, 1998.

2 B. Helms, C. O. Liang, C. J. Hawker and J. M. J. Fréchet, *Macromolecules*, 2005, **38**, 5411–5415; B. Helms, S. Guillaudeu, Y. Xie, M. Mcmurdo, C. Hawker and J. Fréchet, *Angew. Chem., Int. Ed.*, 2005, **44**, 6384–6387; V. Rodionov, H. Gao, S. Scroggins, D. A. Unruh, A. J. Avestro and J. M. J. Fréchet, *J. Am. Chem. Soc.*, 2010, **132**, 2570–2572.

3 M. Zhao, B. Helms, E. Slonkina, S. Friedle, D. Lee, J. DuBois, B. Hedman, K. O. Hodgson, J. M. J. Fréchet and S. J. Lippard, *J. Am. Chem. Soc.*, 2008, **130**, 4352–4363.

4 E. Huerta, P. J. M. Stals, E. W. Meijer and A. R. A. Palmans, *Angew. Chem., Int. Ed.*, 2013, **52**, 2906–2910; P. Cotanda, A. Lu, J. P. Patterson, N. Petzetakis and R. K. O'Reilly, *Macromolecules*, 2012, **45**, 2377–2384; M. M. Müller, M. A. Windsor, W. C. Pomerantz, S. H. Gellman and D. Hilvert, *Angew. Chem., Int. Ed.*, 2009, **48**, 922–925.

5 A. Laschewsky, J.-N. Marsat, K. Skrabania, H. von Berlepsch and C. Böttcher, *Macromol. Chem. Phys.*, 2010, **211**, 215–221.

6 M. F. Semmelhack, C. R. Schmid, D. A. Cortes and C. S. Chou, *J. Am. Chem. Soc.*, 1984, **106**, 3374–3376.

7 P. Gamez, I. W. C. E. Arends, R. A. Sheldon and J. Reedijk, *Adv. Synth. Catal.*, 2004, **346**, 805–811.

8 J. M. Hoover and S. S. Stahl, *J. Am. Chem. Soc.*, 2011, **133**, 16901–16910.

9 N. Mase, T. Mizumori and Y. Tatemoto, *Chem. Commun.*, 2011, **47**, 2086–2088.

10 C. Parmeggiani and F. Cardona, *Green Chem.*, 2012, **14**, 547–564.

11 E. M. Harth, S. Hecht, B. Helms, E. E. Malmstrom, J. M. J. Fréchet and C. J. Hawker, *J. Am. Chem. Soc.*, 2002, **124**, 3926–3938; S. Hecht and J. M. J. Fréchet, *Angew. Chem., Int. Ed.*, 2001, **40**, 74–91; W. R. Dichtel, K.-Y. Baek, J. M. J. Fréchet, I. B. Rietveld and S. A. Vinogradov, *J. Polym. Sci., Part A: Polym. Chem.*, 2006, **44**, 4939–4951.

12 Y. Koda, T. Terashima, A. Nomura, M. Ouchi and M. Sawamoto, *Macromolecules*, 2011, **44**, 4574–4578.

13 J.-N. Marsat, M. Heydenreich, E. Kleinpeter, H. v. Berlepsch, C. Böttcher and A. Laschewsky, *Macromolecules*, 2011, **44**, 2092–2105.

14 A. M. A. Dias, M. Freire, J. A. P. Coutinho and I. M. Marrucho, *Fluid Phase Equilib.*, 2004, **222–223**, 325–330; J. G. Riess, *Chem. Rev.*, 2001, **101**, 2797–2920.

15 K. C. Lowe, *Comp. Biochem. Physiol., Part A: Mol. Integr. Physiol.*, 1986, **87**, 825–838.

16 T. R. Chan, R. Hilgraf, K. B. Sharpless and V. V. Fokin, *Org. Lett.*, 2004, **6**, 2853–2855.

17 P. S. Donnelly, S. D. Zanatta, S. C. Zammit, J. M. White and S. J. Williams, *Chem. Commun.*, 2008, 2459–2461; D. Schweinfurth, S. Demeshko, M. M. Khusniyarov, S. Dechert, V. Gurram, M. R. Buchmeiser, F. Meyer and B. Sarkar, *Inorg. Chem.*, 2012, **51**, 7592–7597.

18 C. J. Hawker, A. W. Bosman and E. Harth, *Chem. Rev.*, 2001, **101**, 3661–3688.

19 K. Matyjaszewski and J. Xia, *Chem. Rev.*, 2001, **101**, 2921–2990.

20 B. Charleux, J. Nicolas and O. Guerret, *Macromolecules*, 2005, **38**, 5485–5492.